KLOE Note n. 92
March 1994

A measurement of the spatial resolution in square drift cells via the stagger method

G.Finocchiaro

Abstract

An analysis of the data collected at P.S.I. on *prototype 0.1* and *prototype 0.2* is presented. The space-time relation is determined from the drift time distribution and from the space-time correlation. The stagger method is used to measure the spatial resolution, which is found to be within the design specification of $200\,\mu$m.

1 Introduction

A test at P.S.I. has been performed during summer '93 in order to measure the performances of two small prototypes with square cells of the KLOE drift chamber. A detailed description of the prototypes, of the test beam setup and of the trigger and DAQ system is given elsewhere [1]. In fig. 1 the layout of the cell configuration is shown. The arrangement of the prototypes in the beam is given in fig. 2. Tracks coming from below in fig. 1 are defined to have 0° incidence angle, tracks from the right 90°.

Stimulated by the fact that in the early days of the test the MWPC were not working properly, we developed a method for measuring the space-time relation and the spatial resolution based exclusively on the drift time information. This method is presented here, toghether with another one, based as well on the stagger among different cells.

2 The space-time relation

In order to transform the drift time measurement into the space coordinates necessary to fit tracks inside the drift chamber, a space-time relation must be given. In this section we describe the two methods adopted to determine the parameters of the space-time relation.

2.1 The space-time relation from the time spectrum

Making the assumption that the cells are uniformly illuminated by the beam[1], the time spectrum measured in a single cell can be written as

$$\frac{\mathrm{d}N}{\mathrm{d}t} = \frac{\mathrm{d}N}{\mathrm{d}x} \cdot \frac{\mathrm{d}x}{\mathrm{d}t} \simeq \mathcal{K}\frac{\mathrm{d}x}{\mathrm{d}t}. \tag{1}$$

thus being proportional to the drift velocity $\mathrm{d}x/\mathrm{d}t$, which in He-based mixtures is far from being saturated. Choosing therefore a functional form $t(x)$ for the space-time relation, its parameters can be determined from a fit to the cell time spectrum with the function $|\mathrm{d}t(x)/\mathrm{d}x|^{-1}$. The normalisation constant $\mathcal{K}$ can be determined requiring that the number of events between times t_1 and t_2 be equal to the integral of the function between the same extremes.

From previous analysis on prototype 0 [2], it is found that a parabolic approximation of the space-time relation:

$$\mathrm{t} = \mathrm{t_0} + \mathrm{A}(\mathrm{r} - \mathrm{r_{wire}})^2 + \mathrm{B}|\mathrm{r} - \mathrm{r_{wire}}| \tag{2}$$

adequately describes a symmetric field configuration. Parameter B has the simple interpretation of the inverse of the drift velocity near the anode wire (i.e. for high electric fields). The method is illustrated for 3 cells of *prototype 0.1* in figure 3, were the fitting function is the inverse of eqn. 2.

[1]For several runs this is actually true only for the central cells.

Events entering the histograms in fig. 3 pass a selection cut based on the total charge released along the track length inside the cell: an event is defined as 'good' if, for all the 5 cells in the row, the ADC value exceeds the pedestal by 3 sigmas. As can be seen from the ADC spectra in fig. 4, this allows a rather clean selection, since the pedestal and signal peaks are well separated.

A few remarks are in order about the fits in fig. 3:

1. Only parameters A and B of eqn. 2 are fitted: x_{wire} does not play any role here, the drift time being sensitive only to $|x - x_{wire}|$; t_0 is determined (not fitted!) from the initial region of the time spectrum.

2. The fitted parameters are consistent among different cells and with previous measurements [2], although the errors are rather large.

3. Since the assumed functional dependence is symmetric, the fit should be performed in a region sufficiently close to the anode wire, where symmetry is actually expected. Given the measured drift velocity in the gas mixture $90\%He - 10\%iC_4H_{10}$, the maximum drift distance in the cell ($\simeq L/2 \simeq 10\,mm$) correspond to $\simeq (400 \div 500)$ ns drift time, as can be seen from the rather sharp decrease in fig. 3. In this respect, 350 ns is a reasonable limit for the fit. To illustrate this point, a calculation of the electric field as a function of the distance from the *sense* wire for tracks at a) 0°, b) 90° respectively, in cell 13 of *prototype 0.1* is shown in fig. 5[2]. A high degree of symmetry is observed in the first case due to the *field* wires at the sides of the cell. On the contrary, 'up' and 'down' *field* wires are slightly displaced in cell 13 (see fig. 1), which results in the asymmetry of fig. 5b for drift distances ≥ 0.6 mm.

This fit method cannot be applied equally well to any cell configuration. The heaviest limitations are for *prototype 0.2*, due to its particular wire configuration. Referring to fig. 1, clusters originated from a track traversing *prototype 0.2* at 90° see a 'closed' cell, like in *prototype 0.1*. On the other hand, clusters from 0° tracks follow the drift lines of an open cell. The different potential configuration is shown in fig. 6. The drift time distribution for tracks at 0° in *prototype 0.2* is shown for one cell in fig. 7. The cell borders are no longer well defined as in *prototype 0.1*. In fact we did not succeed in fitting *prototype 0.2* time spectra at 0°.

2.2 The space-time relation from the space to time correlation

Having at our disposal a tracking system, the most natural way to study the space-time relation is of course to correlate the measured drift time with the projected distance of closest approach (DCA) of the track to the anode wire. The combined efficiency of the 2 MWPC's is $\simeq 40\%$. Examples of correlations are shown in fig. 8 for both prototypes.

[2] The simulation is done by means of the program GARFIELD [3].

Two effects have to be considered, both related to the intrinsic lower linit of the time distribution near the wire:

1. The finite distance between ionization clusters ($\simeq 800\,\mu$m in He-based mixtures with $\geq$ 90%He) distorts the drift time distribution near the wire (getting far from the wire, the effect levels off according to the Pythagorean theorem). One way to correct for this is to replace the DCA coordinate x with

$$x' = \sqrt{x^2 + (\lambda/2)^2}, \tag{3}$$

   where the mean distance between clusters λ is extrapolated from the measured value to the β of the particle.

2. The resolution of the tracking system smears the DCA distribution[3]. For tracks sufficiently far from the anode wire, the mean value of the time distribution is not affected. On the contrary, for clusters released close to the wire the mean value does change, due to the tails caused by events at relatively large time, but whose reconstructed distance is smeared to small x. We found that the bulk of this effect is accounted for by *fixing* independently the t_0. Actually, if one tries to include t_0 in the fit, its value is overestimated (compare the profile histograms with the scatter plots in fig. 8), and correspondigly overestimated is the drift velocity.

An example of parameters fitted in this way is shown in fig. 9.

3 Spatial resolution

In order to measure the spatial resolution in our prototypes, we compared the spatial measurements in several cells. The main advantage of this method is that one automatically gets rid of both any disalignment with respect to the tracking system and the effect of multiple scattering (the cells are typically few cm. – in He – apart).

The correction for the track slope, mandatory to consistently compare the spatial measurements, can be accomplished in two ways. The first method, illustrated in fig. 10, uses only the drift time information from the prototypes themselves. The plot of the quantity

$$\Delta x_{\mathrm{stag}} = \frac{x(t_1) + x(t_3)}{2} - x(t_2) \tag{4}$$

is shown in fig. 11. Tracks are selected requiring 5 hits in the row of interest and only 1 hit in each column of cells. A hit is defined 'good' if the collected charge is at least 3 sigmas above the

[3] In our case the spatial resolution of the tracking system is of the order of 1 mm, due to the combined effect of the intrinsic resolution of the MWPC's ($\simeq 500\,\mu$m), the material traversed by the low momentum pion beam ($\simeq 600\,\mu$m), and the relative disalignment between the prototypes and the MWPC's.

pedestal, and the drift time is lower than $1.5\,\mu$s. The branches of fig. 11 correspond to different configurations of the track with respect to the 3 cells. The difference in height between two the straight branches is twice the stagger between the mean of cells 11 and 15 and cell 13. Examples of Gaussian fits to $500\,\mu$m slices of these branches are shown in fig. 12. The half-distance between the peaks is 2.15 mm, to be compared with the nominal 2.20 mm. The space scale is therefore correcly reconstructed.

The spread around the mean value is the convolution of the spatial resolution of the 3 cells. An example of a fit to the resolution curve (upper branch of fig. 11) is shown in fig. 13. For each cell the diffusion, the 'instrumental' and the ionization contribution to the spatial resolution have been taken into account. The fitted values are consistent with previous measurements [2]; it has to be noted however that, just because of the stagger, the data reach at most $|r| \simeq (7 \div 8)$ mm from the anode wire, where the sensitivity to the diffusion coefficient is reduced.

The spatial resolution has been measured also correcting for the track slope by means of the MWPC information (for nearby cells the errors induced by the telescope slope is negligible). This method has to be used when measuring the resolution comparing the reconstructed distance in cells where the stagger has not the simple interpretation of fig. 10. The mean value of the residuals is shown in figure fig. 14 as a function of the drift distance. The curve is basically flat (as it has to be) and the residuals are contained inside a $\pm 200\,\mu$m band. This gives an *a posteriori* justification for the correctness of using a symmetric function in our drift cells: only at the very border the asymmetry starts to be apparent.

In figures 15-18 examples are shown of resolution curves from the stagger method for different values of high voltage, angle and beam momentum. In all the configurations the mixture 90%He–10%iC_4H_{10} gives results within design specifications.

4 Conclusions

We analysed test beam data on the 2 square cell prototypes of the KLOE drift chamber. The space-time relation has been determined in two different ways, yelding consistent results. Typical errors on fitted parameters in the most precise determination are $\mathcal{O}((5 \div 10)\%)$. The spatial resolution has been measured for both prototypes, both at $0°$ and at $90°$ and for different beam momenta and operating voltages, and it has been found to be within the design specifications of $200\,\mu$m.

References

[1] The KLOE drift chamber group, *Addendum to the Technical Proposal*, in preparation (1994).

[2] G.Bencivenni, A.Calcaterra, M.Carletti, R.de Sangro, G.Felici, G.Finocchiaro, M.Piccolo, P.Santantonio, *KLOE note*, 79/93 (1993).

[3] Garfield, a drift-chamber simulation program, CERN program library entry W5050.

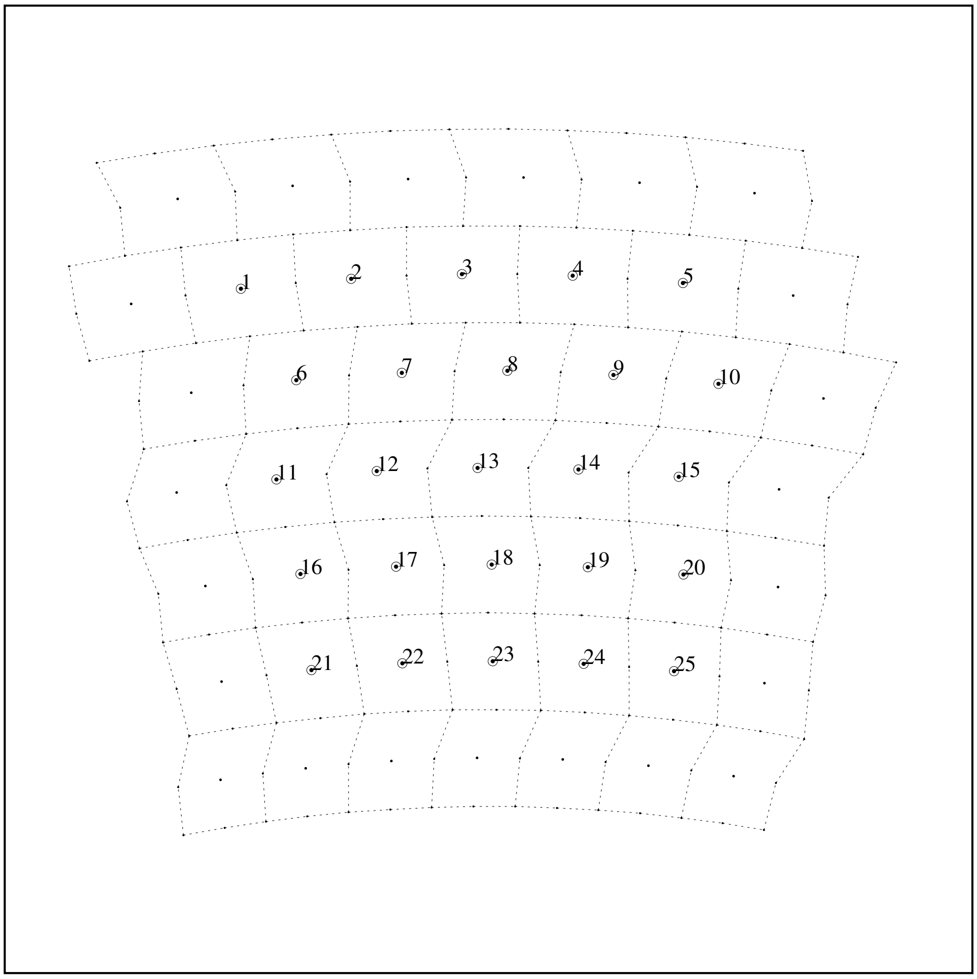

Figure 1: *Sketch of the geometry of* prototypes 0.1 *and* 0.2. *The numbering corresponds to that conventionally assigned to the equipped cells. The field wires on the lateral cell sides are actually there only for* prototype 0.1.

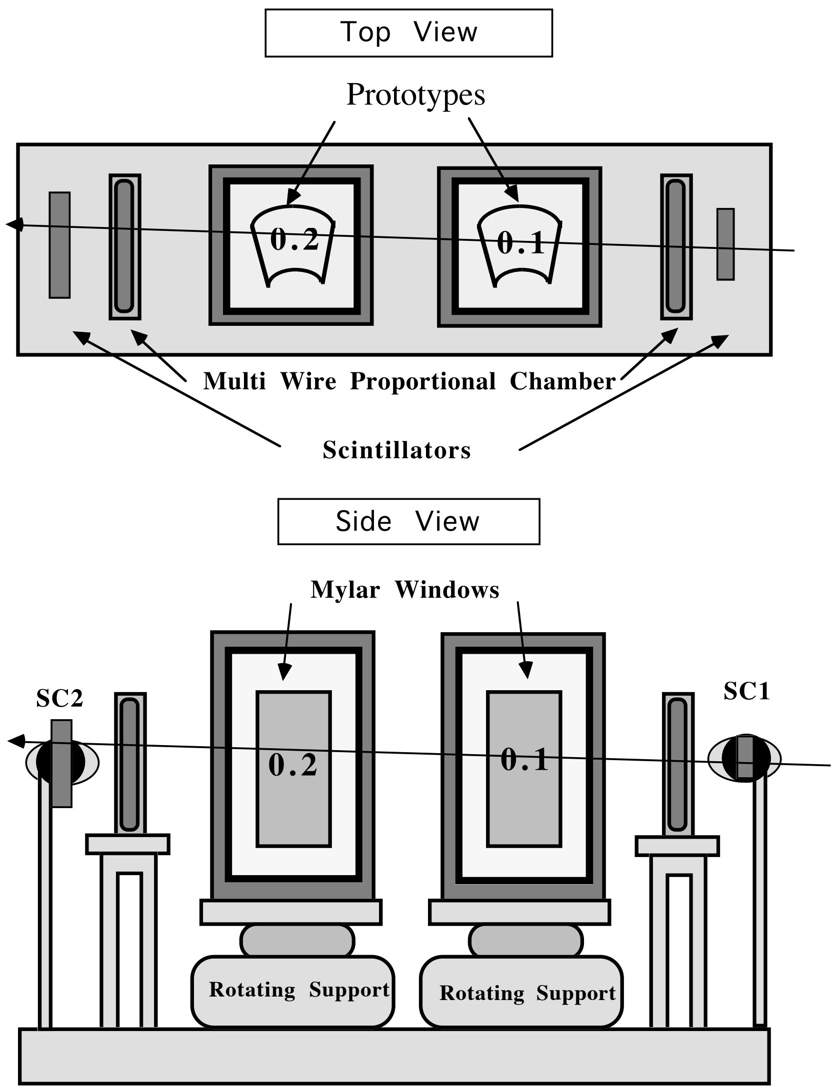

Figure 2: *Scheme of the setup at the P.S.I. test.*

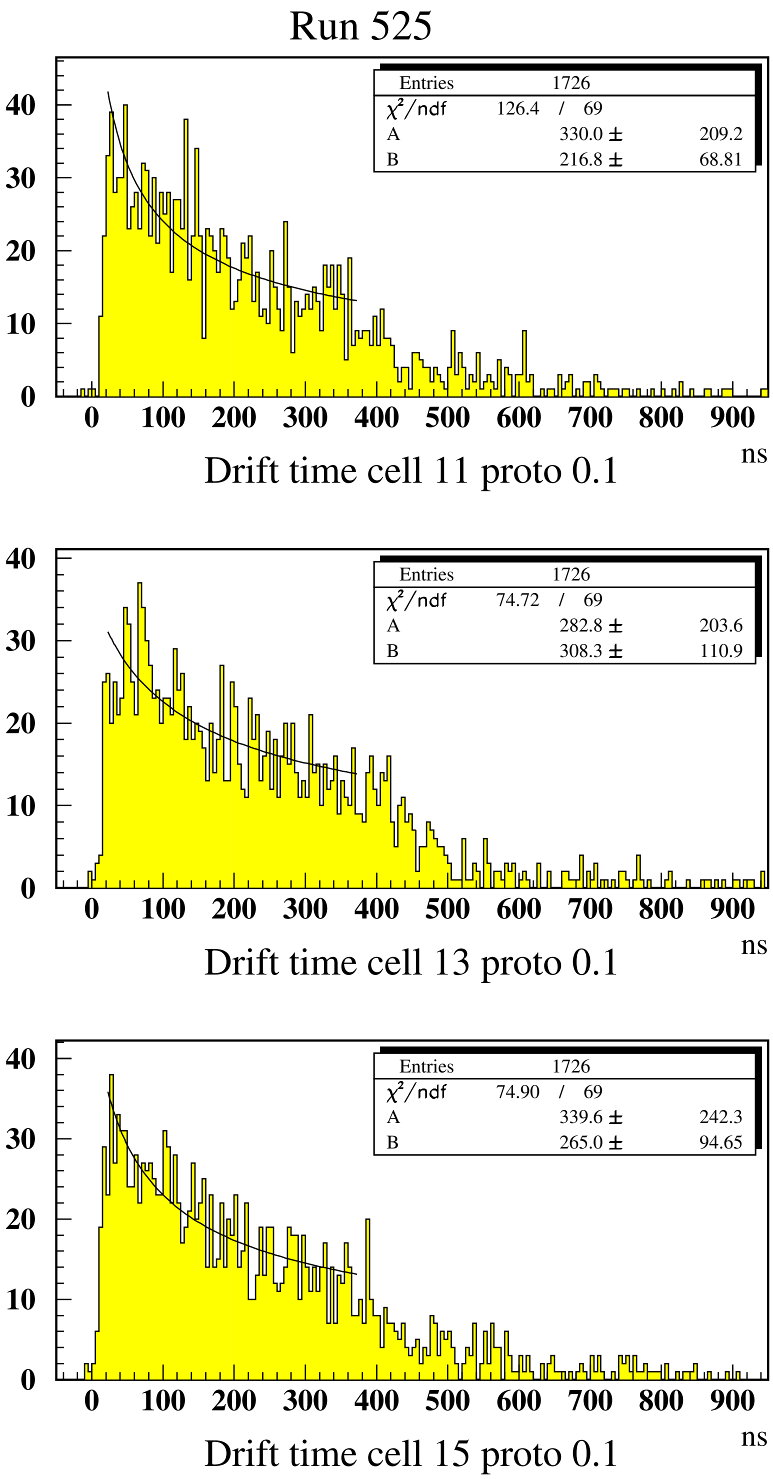

Figure 3: *Parabolic fit to the time spectra for 3 cells of* prototype 0.1. $\phi_1 = 90°$, HV_1*=1800 V. The gas mixture is* 90%He$-$10%iC_4H_{10}.

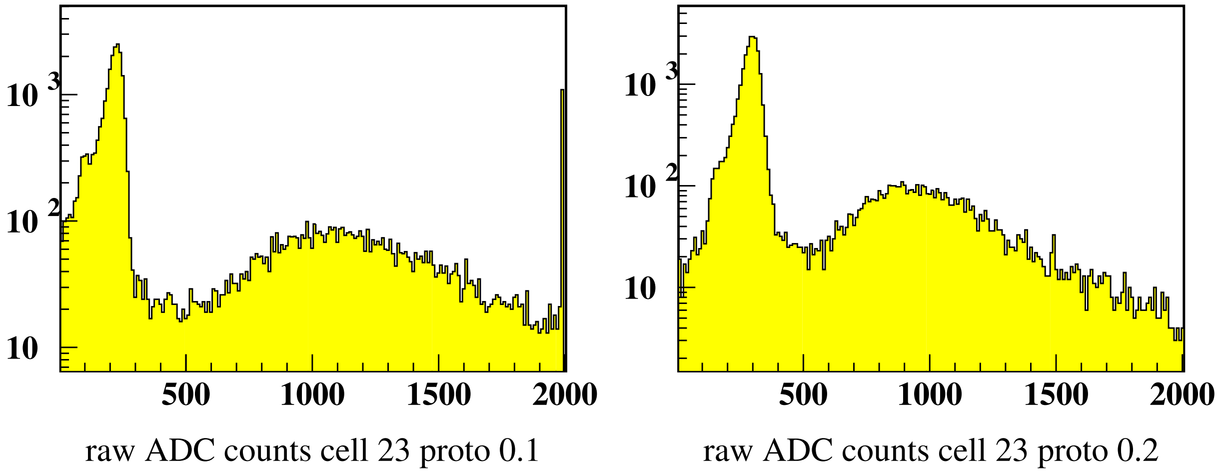

Figure 4: *ADC spectra for one cell in each of the two prototypes.*

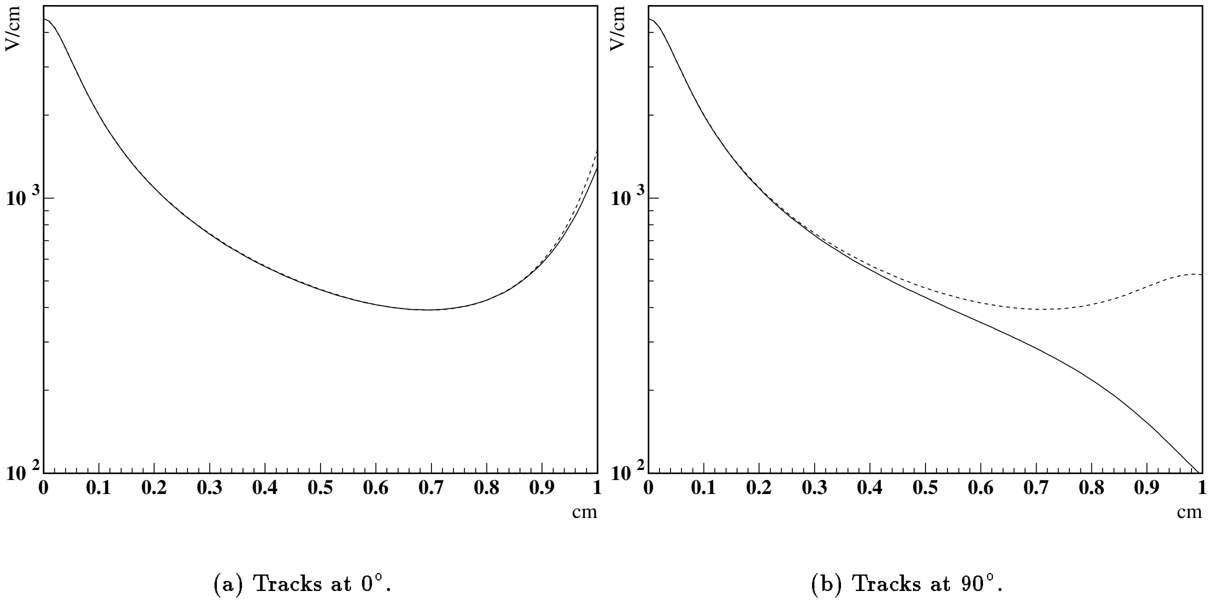

Figure 5: *Profile of the electric field inside cell 13 of* prototype 0.1. *Continuous lines refer to tracks at* x $(y) \geq 0$, *dashed lines to tracks at* x $(y) \leq 0$. *HV=1850 V.*

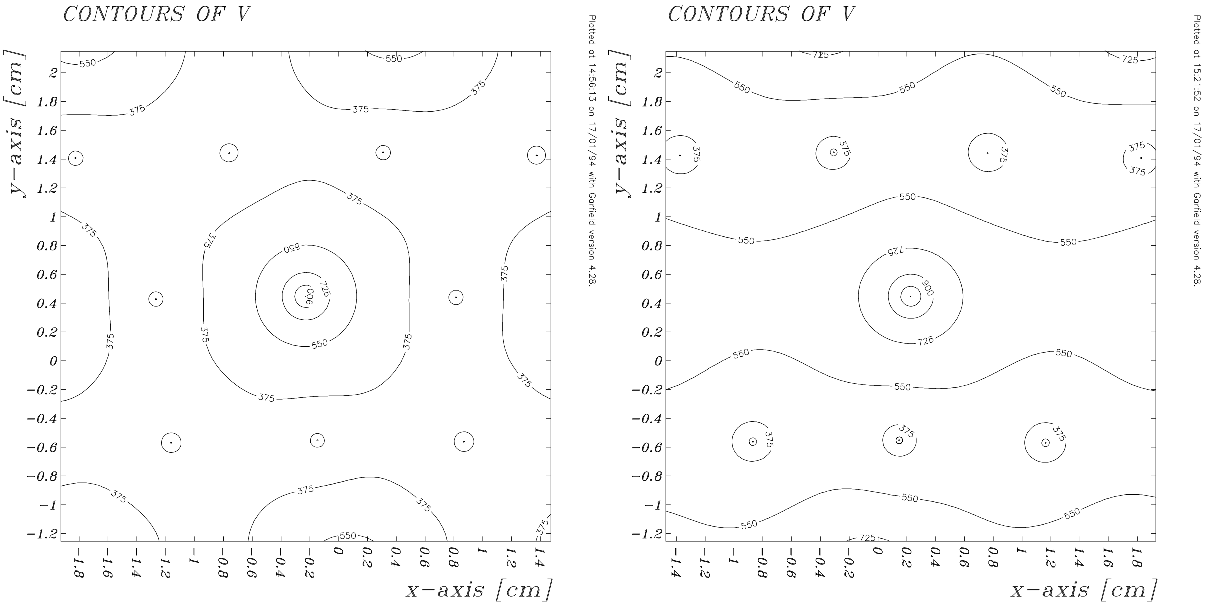

(a) Cell 13, *prototype 0.1*.

(b) Cell 13, *prototype 0.2*.

Figure 6: *Equipotential lines in the 2 prototypes. The 'opening' of* prototype 0.2 *is apparent.*

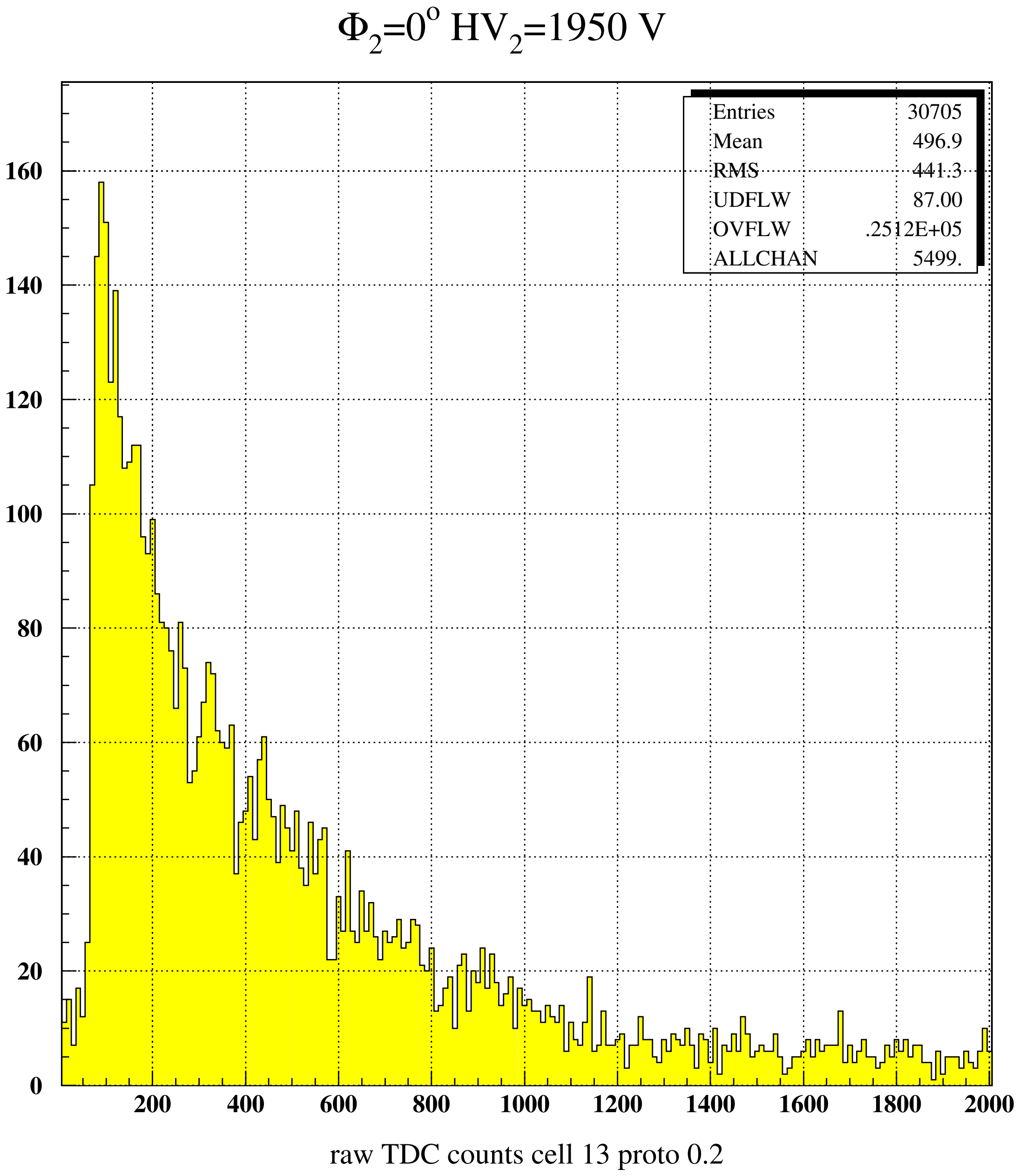

Figure 7: *Time spectrum for 0° tracks in* prototype 0.2.

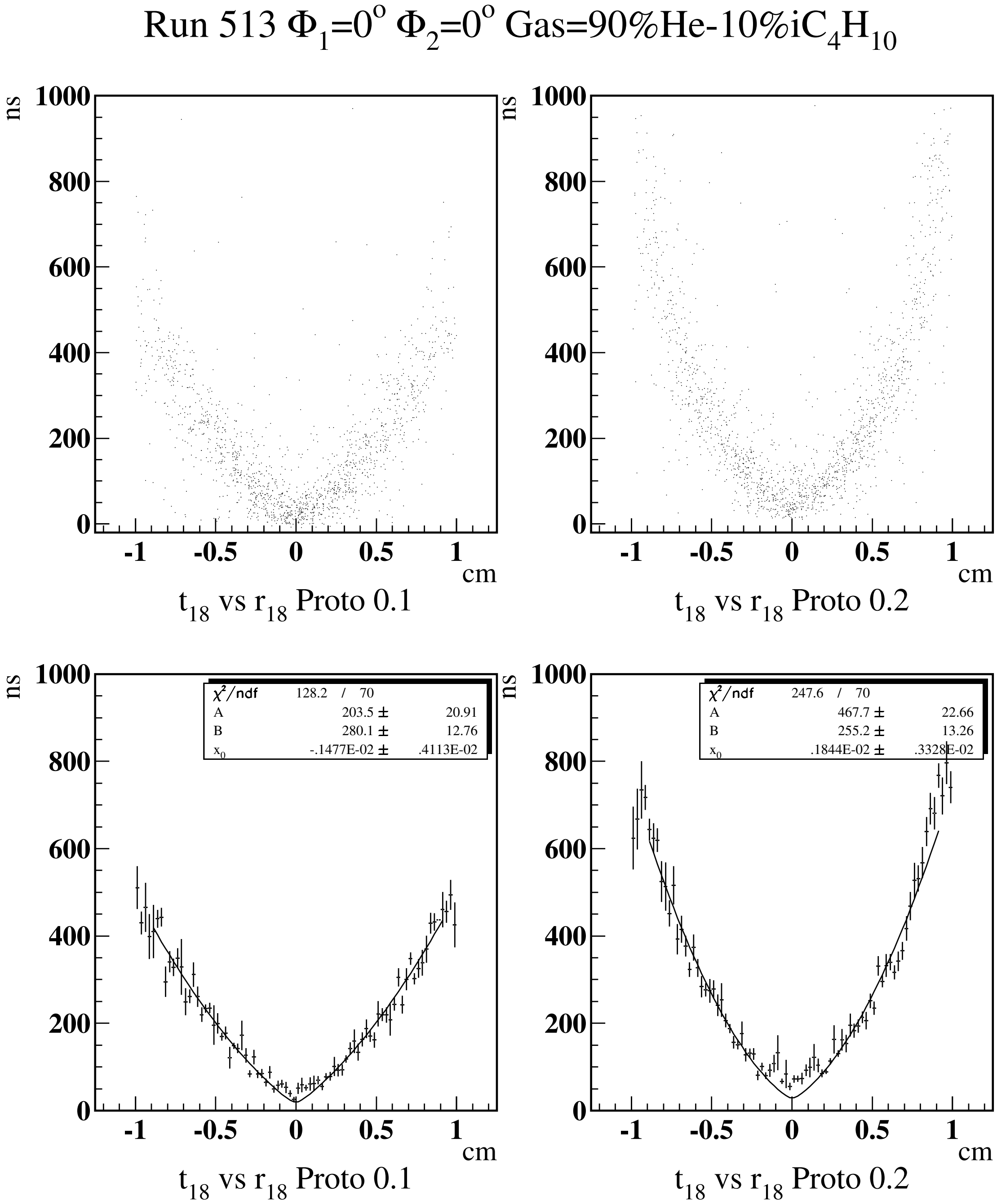

Figure 8: *Space-time relations for the same cell of* prototype 0.1 *and* prototype 0.2. *Near the cell borders, drift times are considerably longer in* prototype 0.2. *Fits with the parabolic function 2, performed in the region* $|\mathrm{r}-\mathrm{r_{wire}}| \leq 0.9\,cm$, *consistently give the same drift velocity close to the wire (1/B).*

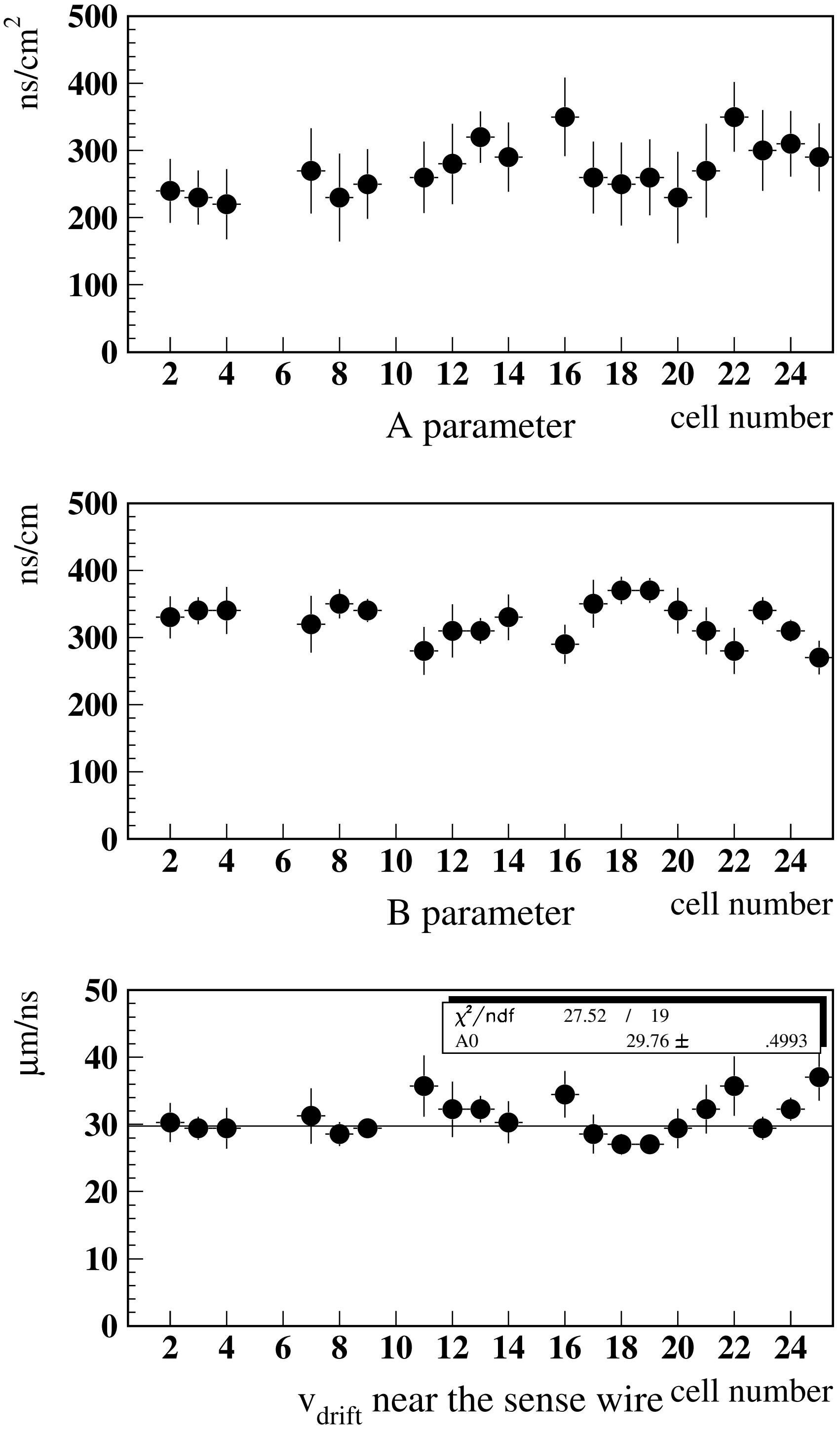

Figure 9: *A, B e drift velocity close to the wire from the parabolic fit for the* prototype 0.2 *cells. Points related to cells non completely illuminated are excluded from the fit.*

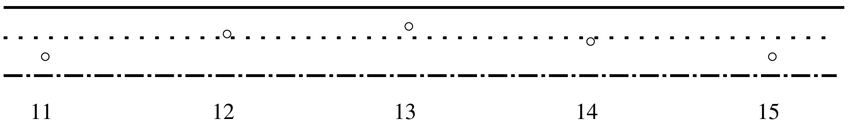

Figure 10: *Illustration of the stagger method using only the time information inside the prototypes. The little circles represent the wire positions in the central row of the prototypes. The lines stand for different track configurations. (see fig. 11.)*

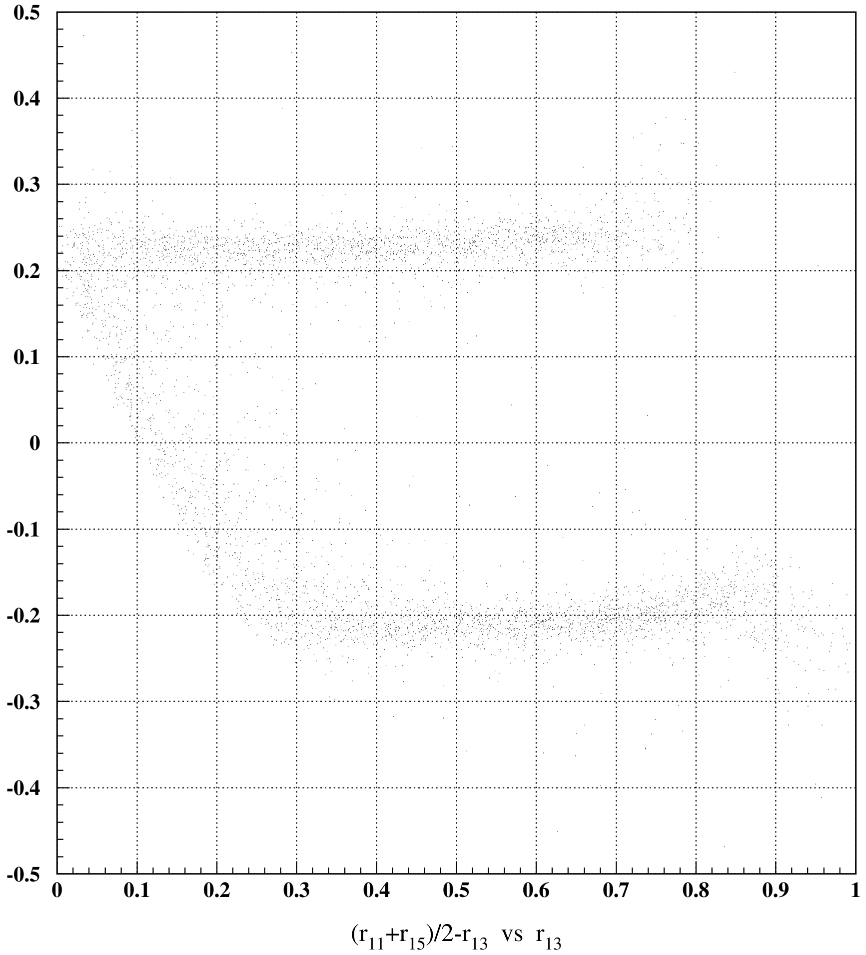

Figure 11: *Scatter-plot of the stagger vs.* r_{13} *(eqn. 4). The upper branch refers to tracks passing like the continuous line in fig. 10, the lower branch to the dashed-dotted line, the branch between them to tracks passed between the central wire and the two lateral ones (dotted line in fig. 10). The scales are in cm.*

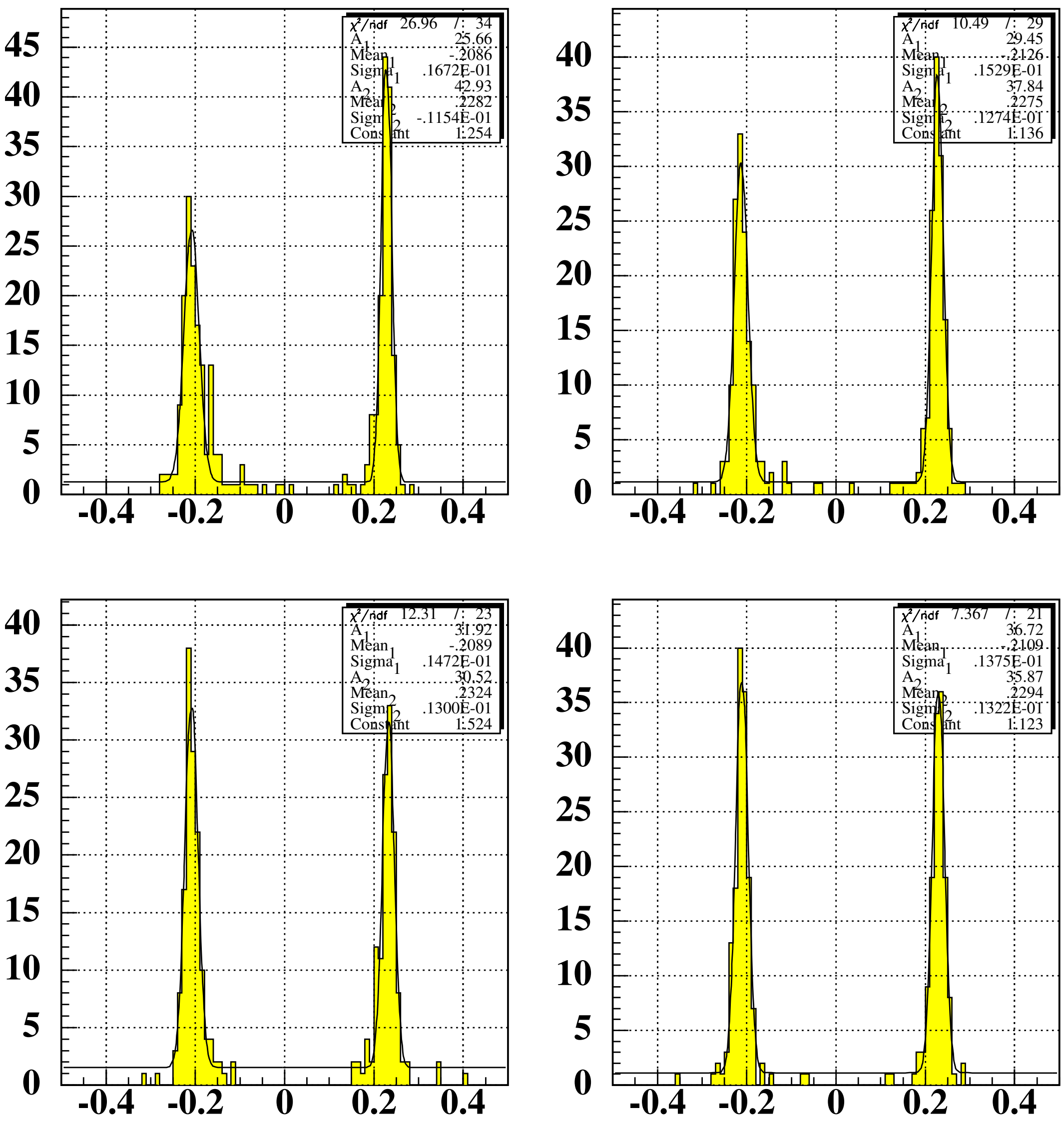

Figure 12: *Gaussian fits to slices ($r_{13} = (4 \div 6)$ mm) of the previous figure. Horizontal scales are in cm.*

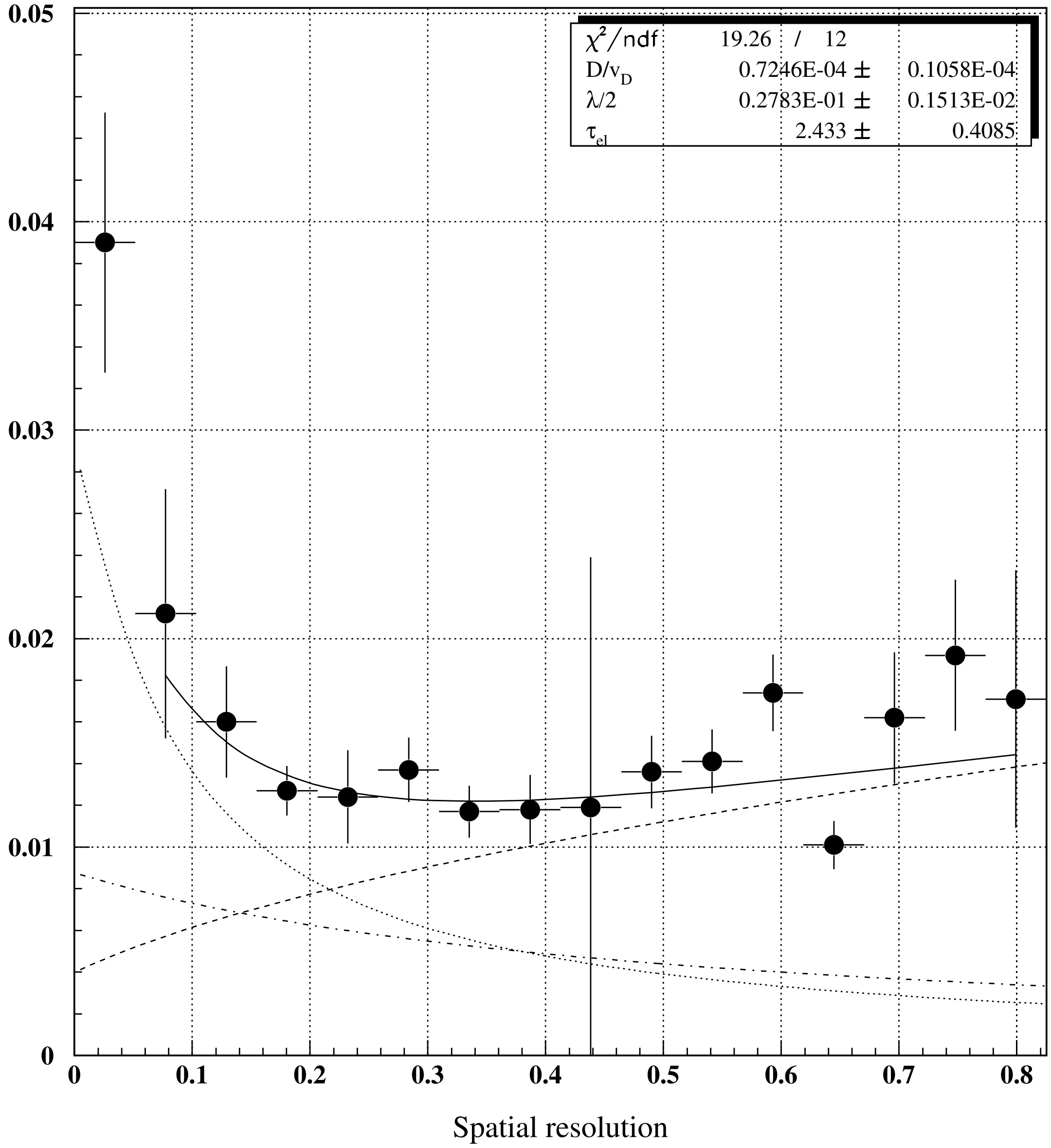

Figure 13: *Fit to the resolution curve for* prototype 0.1. *HV_1=1800 V*, $\phi_1 = 0°$, $p_{beam} = 150\,MeV/c$. *The scales are in cm.*

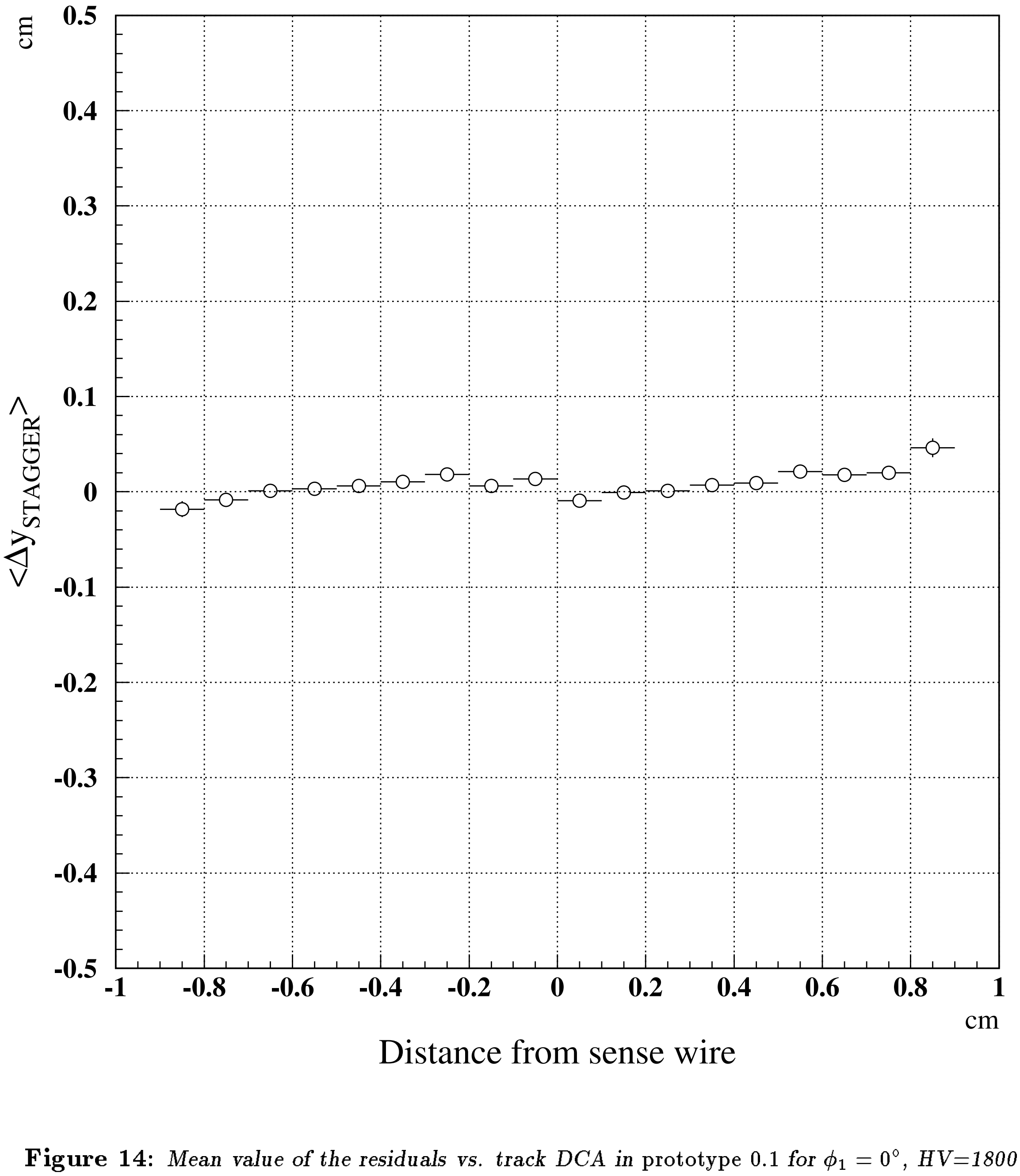

Figure 14: *Mean value of the residuals vs. track DCA in* prototype 0.1 *for* $\phi_1 = 0°$, *HV=1800 V.*

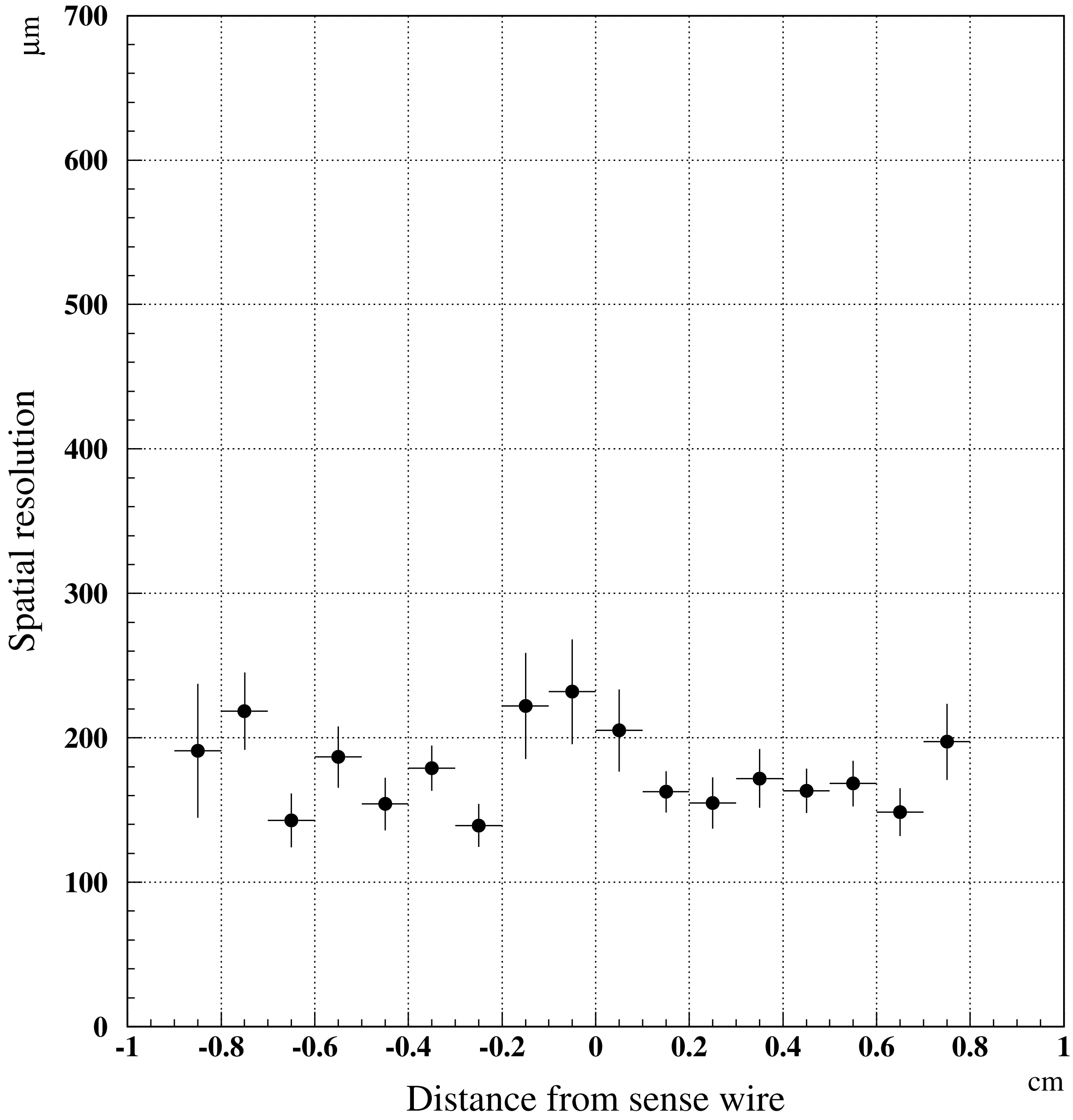

Figure 15: *Resolution curve in* prototype 0.1 *for* $\phi_1 = 0°$, *HV=1800 V*, $p_{beam} = 250\,MeV/c$.

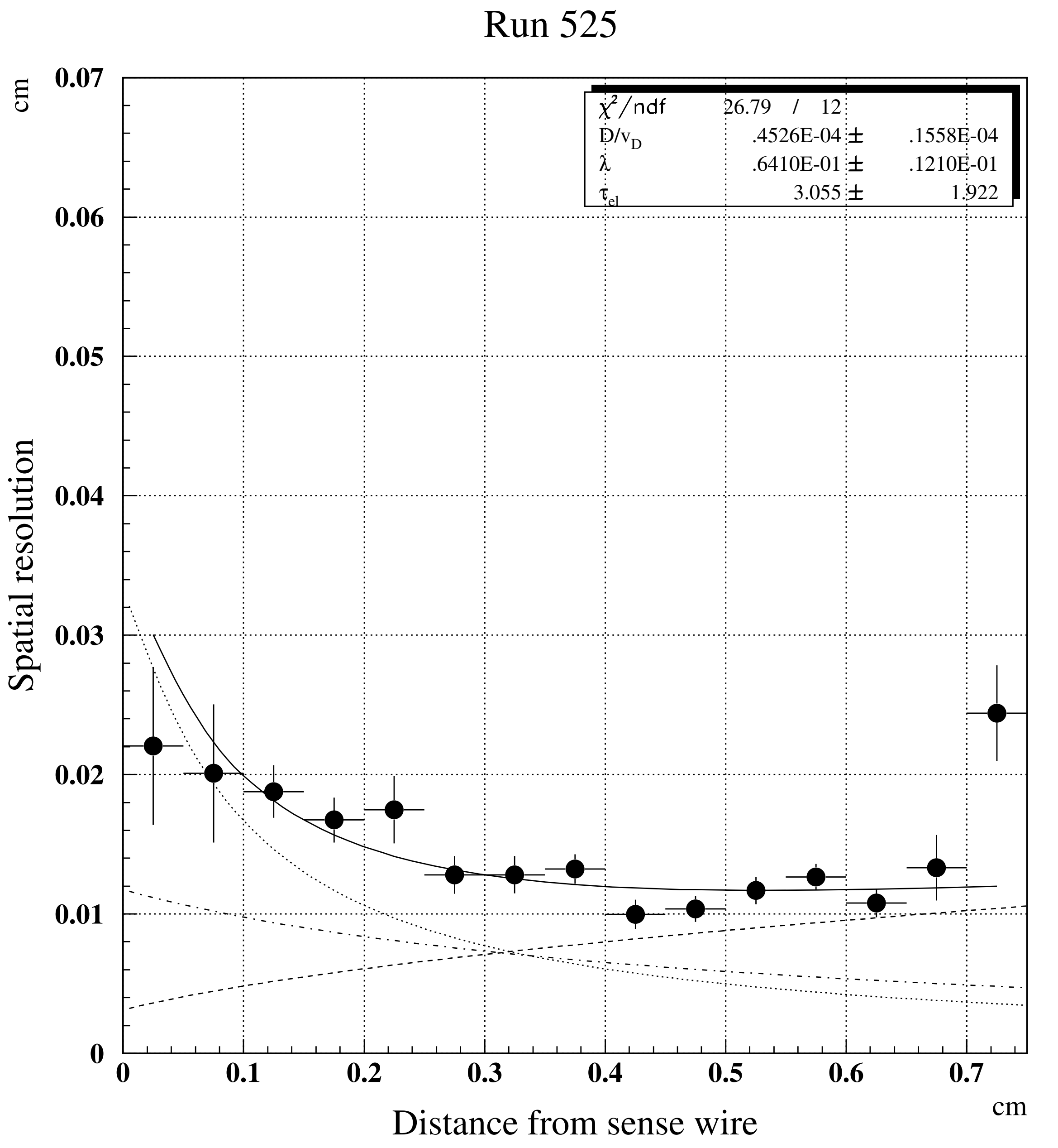

Figure 16: *Resolution curve in* prototype 0.1 *for* $\phi_1 = 90°$, *HV=1800 V*, $p_{beam} = 250\,MeV/c$.

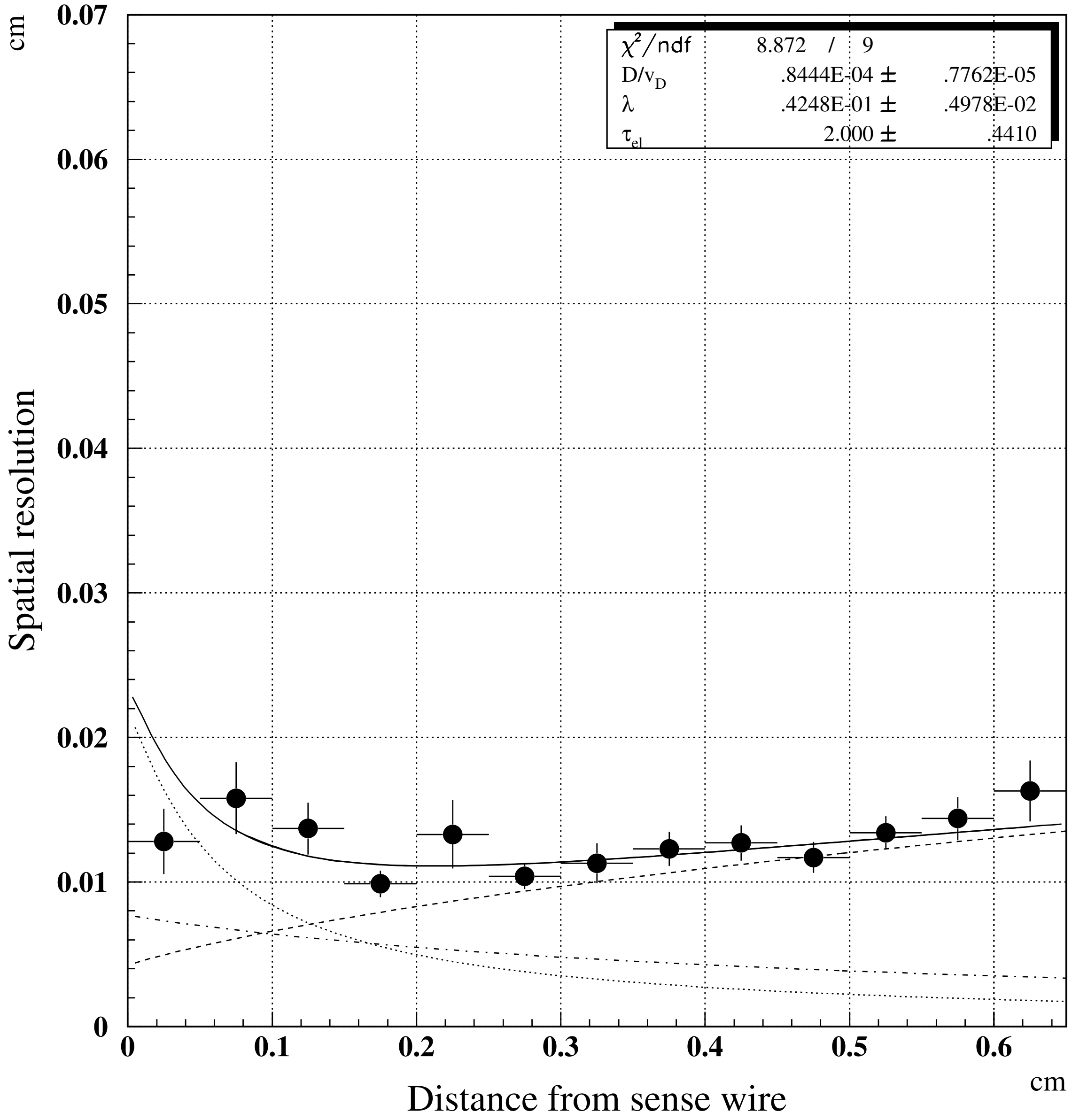

Figure 17: *Resolution curve in* prototype 0.2 *for* $\phi_2 = 90°$, *HV=1950 V*, $p_{beam} = 150\,MeV/c$.

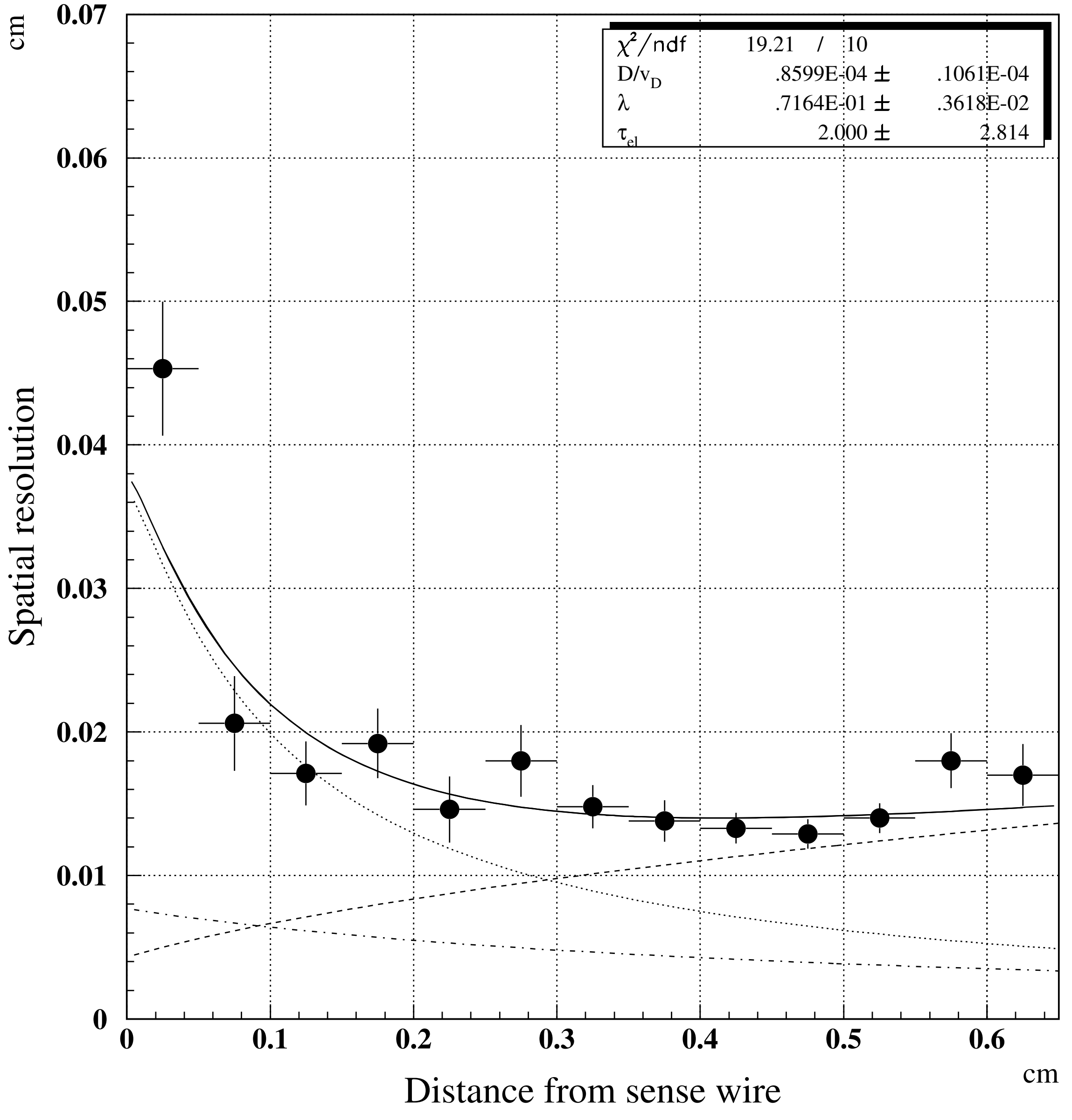

Figure 18: *Resolution curve in* prototype 0.2 *for* $\phi_2 = 90°$, *HV=1950 V*, $p_{beam} = 350\, MeV/c$. *Spatial resolution is marginally worse with respect to previous figure due to the reduced number of cluster/cm released along the track, because of the different beam momentum.*